Airway Morphology From High Resolution Computed Tomography in Healthy Subjects and Patients With Moderate Persistent Asthma

SPYRIDON MONTESANTOS,[1]* IRA KATZ,[1,2] JOHN FLEMING,[3,4] CAROLIN MAJORAL,[1] MARINE PICHELIN,[1] CECILE DUBAU,[1] BENOIT PIEDNOIR,[1] JOY CONWAY,[4,5] JOËLLE TEXEREAU,[1] AND GEORGES CAILLIBOTTE[1]

[1]Medical Gases Group, Air Liquide Santé International, Centre de Recherche Claude-Delorme, Les Loges-en-Josas, France
[2]Department of Mechanical Engineering, Lafayette College, Easton, Pennsylvania
[3]National Institute of Health Research Biomedical Research Unit in Respiratory Disease, Southampton, United Kingdom
[4]Department of Medical Physics and Bioengineeing, University Hospital Southampton NHS Foundation Trust, Southampton, United Kingdom
[5]Faculty of Health Sciences, Southampton UK University Hospital Southampton NHS Foundation Trust, Southampton, United Kingdom

ABSTRACT

Models of the human respiratory tract developed in the past were based on measurements made on human tracheobronchial airways of healthy subjects. With the exception of a few morphometric characteristics such as the bronchial wall thickness (WT), very little has been published concerning the effects of disease on the tree structure and geometrical features. In this study, a commercial software package was used to segment the airway tree of seven healthy and six moderately persistent asthmatic patients from high resolution computed tomography images. The process was assessed with regards to the treatment of the images of the asthmatic group. The *in vivo* results for the bronchial length, diameter, WT, branching, and rotation angles are reported and compared per generation for different lobes. Furthermore, some popular mathematical relationships between these morphometric characteristics were examined in order to verify their validity for both groups. Our results suggest that, even though some relationships agree very well with previously published data, the compartmentalization of airways into lobes and the presence of disease may significantly affect the tree geometry, while the tree structure and airway connectivity is only slightly affected by the disease. Anat Rec, 00:000–000, 2013. © 2013 Wiley Periodicals, Inc.

Key words: bronchial anatomy; asthma; morphometry; high resolution computed tomography; image processing

*Correspondence to: Spyridon Montesantos; Medical Gases Group, Centre de Recherche Claude-Delorme, 1 chemin de la Porte des Loges, B.P. 126 Les Loges-en-Josas, 78354 Jouy-en-Josas Cedex, France. Fax: +33 (0) 1 3907 6199. E-mail: spyridon.montesantos@airliquide.com

Received 10 December 2012; Revised 29 January 2013; Accepted 1 March 2013. DOI 10.1002/ar.22695
Published online in Wiley Online Library (wileyonlinelibrary.com).

The flow of fluids within biological systems has been a subject of increasing research intensity over the past few decades. In the context of gas flow within the tracheobronchial (TB) tree, the delivery of drugs in aerosolized form by inhalation for treating lung diseases or systematic delivery to the blood has necessitated the optimization of this form of therapy. The therapeutic result of such treatments depends on the delivery of aerosols to their intended site of maximum effect. For that reason, a number of studies investigating gas flow (Freitas and Schroder, 2008; Gemci et al., 2008; Lin et al., 2009; Choi et al., 2010; Katz et al., 2011) and aerosol deposition in the lung under various conditions were conducted (van Ertbruggen et al., 2005; Darquenne et al., 2011; Fleming et al., 2011).

A unique aspect of studying biological flows, as opposed to engineering flows, is a lack of precise knowledge of the geometry. Since particle deposition is dependent on the geometric characteristics of the bounding structure within which the gas flows, that is, the airway tree, knowledge of the morphometry of this structure becomes essential. Two principal methods for conducting experimental measurements of the human TB tree have been reported in the literature. The first involves the *ex vivo* evaluation of airway dimensions of lung casts (Weibel, 1963; Horsfield and Cumming, 1967; Horsfield et al., 1971; Phalen et al., 1985) while the second, more modern approach, is the extraction of morphometric information through either High Resolution Computed Tomography (HRCT) (Seneterre et al., 1994; Eberle et al., 1999; Niimi et al., 2000; Sauret et al., 2002; Gono et al., 2003; Tawhai et al., 2004; de Jong et al., 2005; Olivier et al., 2006; Montaudon et al., 2007b; Montaudon et al., 2009; Robinson et al., 2009; Hoshino et al., 2010) or, more recently, through magnetic resonance imaging (Kauczor, 2003; Lewis et al., 2005; Coxson et al., 2009; Peterson et al., 2011). These measurements were often utilized for the creation of anatomical models of either stochastic or deterministic nature (Weibel, 1963; Horsfield and Cumming, 1967; Horsfield et al., 1971; Soong et al., 1979; Yeh and Schum, 1980; ICRP, 1994; Phillips et al., 1994; Fleming et al., 1995; Schmidt et al., 2004; Montesantos et al., 2010). Furthermore, with the help of improved computational techniques, 3D models simulating the bifurcating structure of the airway tree down to various depths were also developed (Martonen et al., 1995; Kitaoka et al., 1999; Sauret et al., 2002; Schmidt et al., 2004; Tawhai et al., 2004; Robinson et al., 2009; Montesantos et al., 2010; Politi et al., 2010).

The ultimate purpose of this line of research is the prediction of gas flow and pharmaceutical aerosol deposition in diseased lungs. Several studies have investigated the transverse structure of individual airways of the upper bronchial tree (Generation 5) and their correlations to the rest of the airway tree (Gono et al., 2003; Kotaru et al., 2005; Olivier et al., 2006; Hoshino et al., 2010) in patients with various asthma severities. These studies mostly concentrate on the bronchial wall thickness (WT) and the lumen area as obtained through lung cast measurements (Wiggs et al., 1992) or medical imaging (Kotaru et al., 2005; Montaudon et al., 2009) and the correlation of these with lung function test parameters (Niimi et al., 2000; Gono et al., 2003; King et al., 2004; Aysola et al., 2008; Hoshino et al., 2010) or with ventilation distribution after methacholin-induced bronchoconstriction (Venegas et al., 2005; Tgavalekos et al., 2007). However, very little information is available concerning the actual changes in geometry and the morphometric relationships of the remodeled airway tree. This has mostly been due to the lack of streamlined, validated processes for the segmentation, and measurement of the bronchi from HRCT images, which is an effect of the unconventional form the airways may take in diseased states.

This article is concerned with the extraction of the morphometric information from the HRCT scans of seven healthy adults and six moderately persistent asthmatic patients through the three-dimensionally reconstructed models of their lungs using the VIDA Pulmonary Workstation 2 (PW2) software package (VIDA Diagnostics, Coralville, IA). The use of this commercial software is explained in some detail because of its growing use as a research tool (Aysola et al., 2008; Tzeng et al., 2008; Coxson et al., 2009). The results were then analyzed to provide insights as to whether there are differences in geometry and connectivity between the healthy and asthmatic populations that extend beyond the lumen diameter and WT. Furthermore, a comparison with the data available in the literature was made in order to assess the consistency of our methods and the validity of some theoretical relationships used for models of the airway tree. Finally, certain aspects of intrasubject variability in different locations within the lung were investigated to evaluate the levels of geometrical nonuniformity at different lung regions in health and asthma.

METHODS

Clinical Study Overview

The HRCT images were captured as part of the protocol of a collaborative research project between Air Liquide Santé International and the National Institute of Health Research Respiratory Biomedical Research Unit of the University Hospital Southampton NHS Foundation Trust (clinical trial EudraCT #2007–003563-43). The study is described in detail elsewhere (Conway et al., 2012). Approval for the study was obtained from the local research ethics committee and the UK Administration of Radioactive Substances Advisory Committee.

In brief, the study included seven healthy subjects and six patients with moderate persistent asthma (GINA guidelines 2005) free from exacerbation for at least four weeks. The recorded FEV_1 values were between 76 and 101%, with daily incidents affecting physical activities. All subjects were male, nonsmokers between the ages of 20 and 58. Demographic and spirometric parameters are available in Table 1. A Siemens Sensation 64 slice HRCT scanner (Siemens, Erlangen, Germany) was utilized to acquire 3D images from the top of the mouth to the base of the lungs. The acquisition was performed with the subject in supine position during slow exhalation against a resistance after a tidal breath. This maneuver was intended to image the glottal aperture in the open position. The imaging parameters were 120 kVp, 120 mAs, and a pitch of 1.0. The average effective dose of radiation for each subject was estimated to be 4.5 mSv. The captured 3D images have slice thickness of 0.75 mm, with pixel spacing varying between 0.55 and 0.65 mm and slice separation of 0.5 mm. The

TABLE 1. Demographic data for the subjects participating in the clinical study

Patient information					
Subject	Age	Height	FRC	FEV_1 (%)	FEV/FVC (%)
H01	24	174	2360	107	98
H02	20	187	4800	115	103
H03	26	177	3170	102	99
H04	20	186	4170	114	99
H05	27	173	3480	91	92
H06	31	179	2910	96	95
P04	45.5	173	2800	107	106
A01	36	174	4650	100	89
A02	42	177	3270	102	95
A03	20	188	4550	89	80
A04	20.5	182	3910	101	87
A05	58	187	3810	76	80
A06	40	180	3380	85	83

The age (years), height (cm), FRC (ml), FEV_1 (%), and FEV_1/FVC (%) were recorded. All subjects are male.

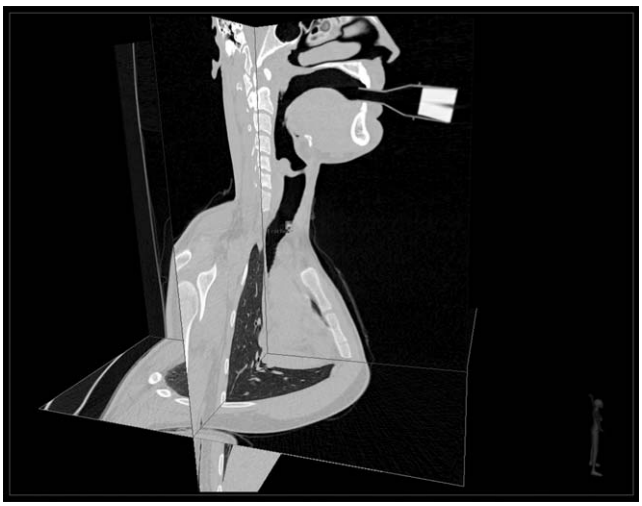

Fig. 1. An example of a composite transverse, coronal and sagittal HRCT image of the full respiratory tract including the mouthpiece, oropharynx, and the lungs for subject H01.

PW2 software was used for the image analysis and reconstruction. MATLAB software version 7.10 and SAS v9.2 were used for data processing and analysis. The HRCT images (Fig. 1) will be available in DICOM format at www.southampton.ac.uk/srig.

Bronchial Geometry Acquisition

PW2 allows for the semiautomatic segmentation and the 3D reconstruction of the human airway tree and the lung space as acquired by CT images. The first part of the process involves the acquisition of the bronchial tree and begins the segmentation of the air-path from the HRCT data using a filling algorithm. Because the software was not designed to treat the extra thoracic region, a seed must be manually placed at the carina to identify the main bronchi if it is present in the DICOM images; otherwise, the process is performed automatically.

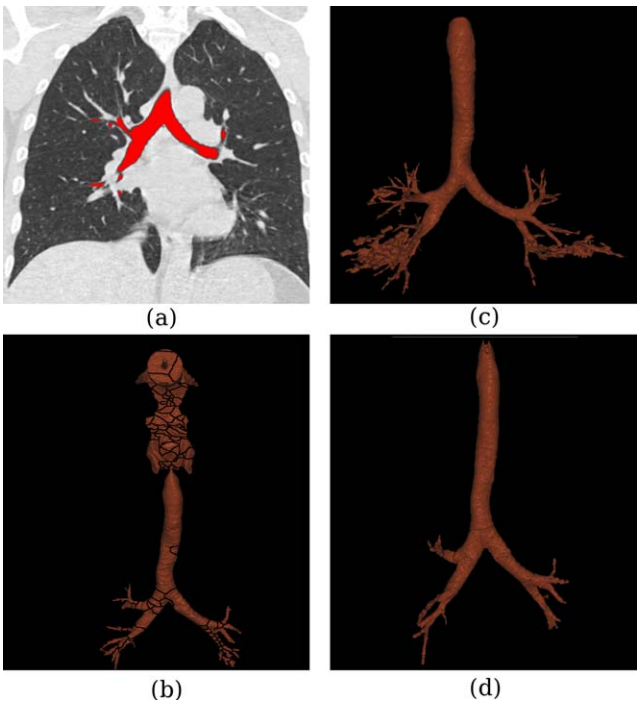

Fig. 2. **a**) Airway masks on a coronal HRCT slice. **b**) Effects of multiple-path segmentation. The ET region, where such effects are more prominent, is also visible. **c**) An example of leakages during segmentation. **d**) Incomplete tree as seen prior to manual correction. Segments in b) and d) are visibly separated

The optimal output from this process is a single, bifurcating, or trifurcating volumetric representation of the tree; at this point, no unique identification of any distinct airways exists. This is available either as a 3D reconstruction of the volume or through a 2D mask placed on the HRCT images along each axis (Fig. 2a). The routine, however, is often affected by uncertainties of airway wall boundaries caused by noise or simply a lack of resolution. The former usually creates multiple interconnected segments, which make for a very nonrobust tree structure (Fig. 2b) while the latter produces uncontrolled leakages of the airway mask to the parenchyma region (Fig. 2c). Noise artifacts were treated through filtering while leakages were removed manually.

The automatic segmentation was generally effective for bronchi between Generations 1 and 5. Therefore, a number of airways that had to be added to the structure, even though they were previously unsegmented by the automatic routine, were visually identified. These existed mostly at the more “noisy” regions of the lung, such as the left lower lobe (LLL) where the heart motion increases image blurring. The airway addition was done either by manually masking regions on the 2D slices, or by seeding unsegmented points of the airway tree and then locally reapplying the automatic segmentation routine. Attention was given to the fact that the resulting supplementary airways must be connected to their respective parents. Additionally, they must be continuous and as robust as possible. For optimal results, a combination of both techniques was usually necessary; for the

healthy subjects, airways down to Generation 9 (right lower lobe [RLL]) were typically attainable. Special consideration was given to the scans of the asthmatic patients, where several artifacts such as airway stenoses, higher radii of curvature, or increased image noise were present (Fig. 3). In the case of stenoses, it was sometimes necessary to generate thread-like connection to parent airways using the manual tools provided by the program.

Following the segmentation of the skeleton, that is, the central path of the resulting volumetric airway tree, was calculated. This was created using a 3D volume erosion algorithm and consists of the voxel-wide core of the airways between branches. The skeleton of the tree is required for the purpose of differentiating between bronchi, thus enabling the program to make the necessary morphometric computations per airway. The skeletonization process itself seemed to interact well with the 3D segment and is fully automatic. However, both siblings of an airway pair need to have enough length in order to be uniquely identifiable. For that reason, in cases of very high asymmetry, in some types of trifurcations, in highly irregular structures such as the ones present in disease or, finally, in lung depths where the airways have insufficient length, the technique failed to distinguish between separate paths. In such instances the whole resulting subtree was erased.

The anatomic labeling of the airways was based on the standard atlas of PW2. Each airway was assigned a unique identification number and, for airways down to the sublobar level, an anatomic name also. The atlas assumes 10 sublobar regions for the right lung and nine for the left lung; the airways were named accordingly based on relative position and connectivity criteria. Due to strong intersubject variability a number of airway trees deviated from the standard atlas. Therefore, the automatic method sometimes failed to recognize the correct bronchi. As the computation routines of certain features such as airway generation are affected by labeling, manual renaming of the airways was performed prior to the automatic measurements of bronchial geometry.

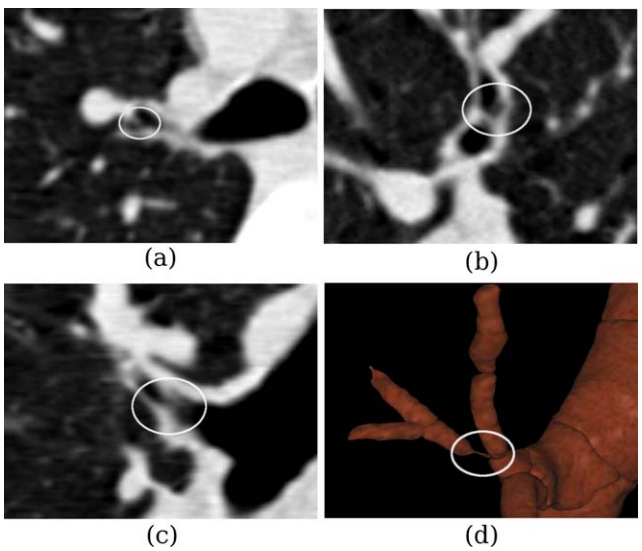

Fig. 3. HRCT of an asthmatic patient displaying an uncharacteristic airway stenosis in the RUL (third generation). The region of interest is marked with a circle and is shown from different perspectives: **a**) transverse, **b**) coronal, **c**) sagittal, and **d**) 3D reconstruction.

Lung Volume Acquisition

The PW2 software was also used to obtain the lung and lobar volumes. The lung position in the 3D space was defined by the reconstructed tree, and an automatic routine was used for the identification of the lung space. The hilar lung region is very irregularly shaped (Fig. 4a) because of the increased tissue and blood-vessel concentration in this region. As this had the effect that some centrally located airways were calculated to be outside of the estimated lung volume, a number of manual corrections were required. The intervention was performed via masking the relevant regions of interest (ROI) directly on the HRCT slices. A smoothing filter was then applied to ameliorate the abrupt shape changes and impose a degree of regularity on the lung outline (Fig. 4b).

The extraction of the lobar volumes was semiautomatic and involved the identification of the main lobar blood vessels (automatically or manually) and the intralobular fissures. The resulting lobar masks were available for examination by the user, in both 2D and 3D (Figs. 5a,b). In the case where the software failed to

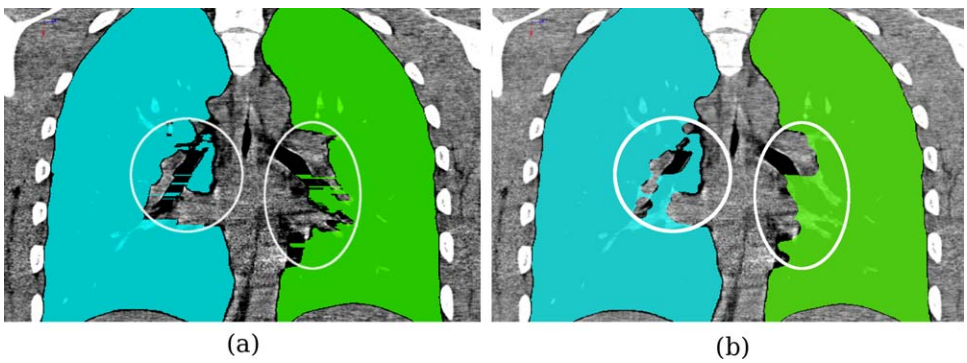

Fig. 4. Automatic extraction of lung space in HRCT. **a**) Raw extraction and **b**) smoothed lung space. The masks are shown in lightly transparent blue (right lung) and green (left lung) and the ROI are surrounded by circles.

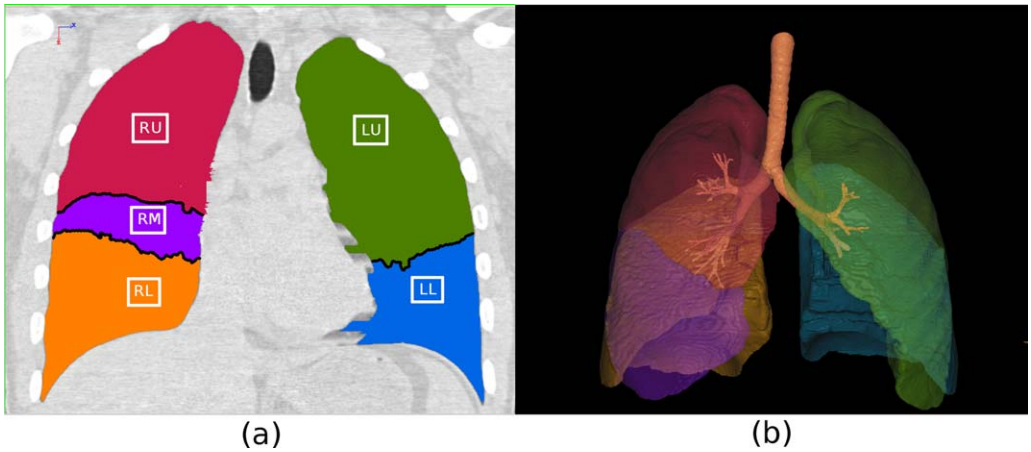

Fig. 5. **a**) 2D coronal representation of the right upper (RU, red), middle (RM, purple), lower (RL, orange), left upper (LU, green), and left lower (LL, blue) lobes. **b**) A 3D view of the completely segmented airway tree along with the lobar regions of the lung.

segment the lobes realistically, an alternative technique was available for dividing the volume of each lung into three subdivisions of roughly equal dimensions. However, this was not considered necessary for any of the subjects under investigation. A combined view of the bronchial tree along with the realistic lung lobes can be seen in Fig. 5b. The investigation of sublobar spaces was not in the scope of this study and, for that reason, lobar subdivision was not pursued.

RESULTS

Structural Variability

Figures 6a,b are three-dimensional illustrations of the structural intersubject variability inherent to the human lung. In Fig. 6a, different possible arrangements of the right upper lobe (RUL) in healthy individuals are shown. Similar variabilities were also found in right middle lobe (RML) and RLL (Fig. 6b). On some occasions, even the anatomical characterization of the bronchi was not uniquely identifiable. For example, see the unexpected trifurcation present at the sublobar level of the RML (airways marked as T1, T2, and T3) in Fig. 6b.

More specifically, the classification of the bronchi revealed that the most frequent segmental configuration of the RUL was a trifurcation (3/7 healthy and 3/6 asthmatics), with the second most frequently observed being the combination of the superior-posterior (RB_{1+2}) to the Anterior (RB_3). Two trifurcations were observed at the segmental level of the RML, both on the healthy subjects. The right subsuperior (RB*) segment is visible in 3/7 healthy and 5/6 asthmatics, while the left RB* was only observed in 3/7 healthy subjects. Finally, a variety of configurations was also observed in the basilar segments of the LLL, with the most common being the bifurcation between the anteromedial basilar (RB_{7+8}) and the lateral-posterior basilar (RB_{8+9}) segments (2/7 healthy and 5/6 asthmatics).

Table 2 displays the number of delineated airways per generation against the total number of airways expected, if the airway tree is considered a strictly bifurcating structure (first number within parenthesis, the trachea being Generation 0). It can be seen that a successful delineation of airways is possible at 74.1% of Generation 5 airways for the healthy and 62.5% of the asthmatic patients, while these percentages drop to 26.8% and 10.4%, respectively for Generation 6. Furthermore, the presence of trifurcations, which were collected and listed also in Table 2 (second number in parenthesis), increases the number of airways measured as compared to a bifurcating model, especially in the more central portions of the lung where all the airways are expected to be recognized and segmented.

There are occasions where an anatomical trifurcation is reconstructed by the PW2 software as two consecutive bifurcations (subject H03, Fig. 6a), with the use of a small, “intermediate” branch. These intermediate branches were also recorded along next to the trifurcations per airway generation for each lobe of each subject in Table 2 (third number in parenthesis). It can be observed that trifurcations, either simulated (with the use of intermediate branches) or labeled as such, can be commonly found below Generation 5 in the RLL and Generation 4 in the LLL. The RUL was more prone to present trifurcating structures than the left upper lobe at the segmental level, especially for the asthmatics.

Airway Morphometric Measurements

The main morphologic characteristics of the bronchial tree (diameter (D), length (L), branching angle (θ), planar rotation angle (φ), and average WT) are displayed in Table 3 for each generation and lobe, separately for the healthy and the asthmatic subjects. D and WT are the average values measured along the length of a segmented airway, L is the distance between start and end bifurcation points, and θ is the angle between parent and daughter branches, each defined as a straight line. Finally, φ is the angle between the parent and daughter planes. In trifurcations, two φ angles are measured, that between the largest and middle diameter airways and the one between the middle and smaller diameter airway. The values for the trachea, the main bronchi, and the right intermediate bronchus are provided separately, since they do not belong to any lobe. The definition of

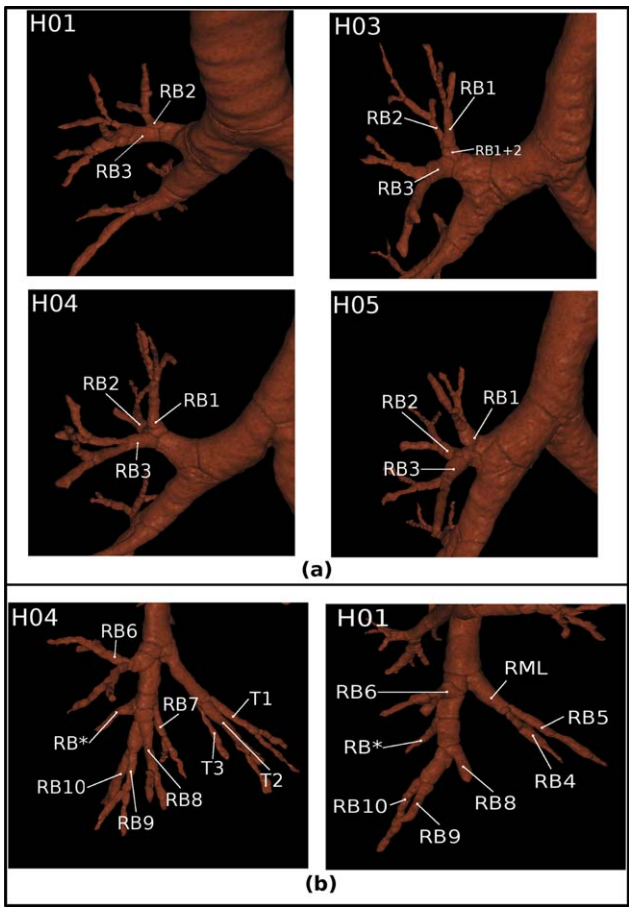

Fig. 6. **a**) A representation of intersubject variability, as displayed in the sublobar airways of the RUL of healthy subjects (H01, H03, H04, and H05). RB1, RB2, and RB3 denote the right upper apical, posterior and anterior bronchopulmonary segments respectively. RB_{1+2} points to an intermediate airway. **b**) A representation of intersubject variability, as displayed in the sublobar airways of the right middle and lower lobes of healthy subjects (H01 and H04). RB4 and RB4 are the right middle lateral and medial segments, while RB6 to RB10 are the right lower superior, anterior-basal, medial-basal, lateral-basal, and anterior-basal bronchopulmonary segments respectively. RB* is the right subsuperior bronchus. Finally, T1 and T2 are the medial and lateral bronchi of a RML trifurcation and T3 represents an unidentifiable member of the trifurcating structure.

airway generation used is the one introduced by Weibel, 1963, assigning a generation to all polyfurcating airways, including the "intermediate" ones.

The data in Table 3 reveal that the two clinical-study groups display similar trends for the separate lobes, with only the RML showing different behavior for the length and branching angle. It can be seen that the RLL Generation 3 bronchi are smaller in length but larger in diameter than the rest of the lobes. The average diameter per generation declines exponentially, with the diameter 25% higher in the RUL and RLL of the healthy group down to Generation 6, where a convergence to the same airway scale occurs. There is a large θ in the root airways (defined as the first airways giving rise to distinct subtrees) of the upper lobes (between 55° and 65°), which then declines to between 30° and 35° at Generation 6 (standard deviation is steady at 10°). The pattern is different for the RML, where the theta gets close to 20° at Generations 5 and 6. The intersubject variability is considerable, with the average coefficient of variation calculated from Table 3 between 17% for D and 29% for θ. Finally, a visible trend for higher WT exists in the asthmatic group. The average values per generation are compared to literature results in the graphs of Fig. 7.

Certain important morphometric relationships available in the literature were also investigated, and the results are presented per lobe for the healthy and asthmatic subjects in Table 4. The homothety ratio (HR), that is, the ratio of the diameters of two consecutive generations (Montaudon et al., 2007a) was obtained using the relationships

$$D_{(j+1)} = D_j * HR \tag{1}$$

$$D^{MAJOR}_{(j+1)} = D_j * HR_{MAJOR} \tag{2}$$

$$D^{Minor}_{(j+1)} = D_j * HR_{Minor} \tag{3}$$

where D is the diameter, j is the Weibel generation, and eqs. (2) and (3) examine the HR for the parent-major daughter and parent-minor daughter pairs, respectively. It can be observed that, even though some intralobe differences might exist between the healthy and the asthmatic subjects (for example, the major daughter of the RML and RLL), the average HR values are very similar between the two groups.

A least squares linear regression analysis examining the characteristics of the line that best fits the HR data obtained in this study was performed in order to assess the quality of the linear relationships provided by eqs. (1–3), with the results displayed in Table 4. The relationship holds relatively well for the healthy group, with an average determination coefficient $R^2 = 0.7$, which is much better than the asthmatic group (average $R^2 = 0.51$). The latter is heavily affected by the very bad fit of the linear model of the two lower lobes. Furthermore, the R^2 is consistently higher for the major daughter subgroup (average of 0.73 and 0.63 for the healthy and the asthmatic groups, respectively) than in the minor daughter subgroup (average of 0.66 and 0.51). The length-to-diameter (L/D) ratio was also calculated for each lobe (Table 4). The average values are almost equal between the two groups with $L/D_{healthy} = 2.72 \pm 1.48$ and $L/D_{asthmatic} = 2.69 \pm 1.25$.

Statistical Analysis

A series of analysis of variance (ANOVA) tests were performed between the morphometric parameters of the healthy and asthmatic groups in order to verify if the differences noted between them are statistically significant. The difference in average WT proved to be statistically significant ($mean_{diff} = 0.12$ mm and $P < 0.001$). The rest of the data displayed no statistically significant differences between the two groups, with the exception of the logarithm of D, which is borderline significant ($P = 0.066$).

The Pearson correlation coefficient (r) was calculated between the morphometric parameters for each lobe

TABLE 2. The number of airways per generation detected from the HRCT images of a) seven healthy and b) six asthmatic subjects

		Airway structure and interconnection information					
	Gen	RUL	RML	RLL	LUL	LLL	% of bronchi detected
(a) Healthy Subjects	2	7 (7,0,0,0)	–	–	7 (7,0,0,0)	7 (7,0,0,0)	100,0%
	3	15 (14,1,1,0)	7 (7,0,0,0)	7 (7,0,0,0)	14 (14,0,0,1)	14 (14,0,0,2)	101,7%
	4	30 (28,0,0,1)	14 (14,1,0,7)	14 (14,0,0,1)	26 (28,1,0,10)	29 (28,2,3,12)	100,8%
	5	56 (56,1,0,41)	18 (28,0,0,12)	26 (28,4,0,6)	32 (56,1,0,20)	34 (56,1,0,27)	74,1%
	6	30 (112,2,0,27)	12 (56,1,0,12)	40 (56,3,0,27)	24 (112,1,0,21)	14 (112,1,0,11)	26,7%
	7	6 (224,0,0,6)	–	26 (112,2,0,11)	6 (224,0,0,6)	6 (224,0,0,5)	4,9%
	8	–	–	31 (224,0,1,19)	–	2 (548,0,0,2)	1,8%
	9	–	–	24 (548,1,0,20)	–	–	0,6%
	10	–	–	8 (1096,0,0,8)	–	–	0,1%
(b) Asthmatic Patients	2	6 (6,0,0,0)	–	–	6 (6,0,0,0)	6 (6,0,0,0)	100,00%
	3	12 (12,4,0,0)	6 (6,0,0,0)	6 (6,0,0,0)	12 (12,0,0,0)	12 (12,0,0,2)	100,00%
	4	24 (24,1,0,3)	12 (12,1,0,7)	12 (12,0,0,1)	24 (24,2,0,13)	22 (24,4,2,11)	97,9%
	5	44 (48,0,2,40)	10 (24,0,0,10)	22 (24,3,0,13)	22 (48,0,0,9)	22 (48,0,0,18)	62,5%
	6	8 (96,0,0,8)	–	18 (48,3,0,9)	6 (96,0,0,6)	8 (96,0,0,7)	10,4%
	7	–	–	18 (96,0,0,10)	–	2 (192,0,0,2)	2,6%
	8	–	–	16 (192,0,0,11)	–	–	1,0%
	9	–	–	10 (384,1,0,9)	–	–	0,3%
	10	–	–	2 (768,0,0,2)	–	–	0,0%

In the parentheses are given i) the expected number of airways in a strictly bifurcating structure, ii) the number of intermediate airways, iii) the number of trifurcations, and iv) the number of paths terminating in each generation.

separately to investigate if there appears to be any strong linear correlation between them (Fig. 8). A moderate correlation ($0.4 \leq r \leq 0.7$) between D and WT was observed for the five lobes, with r between 0.31 in the LLL and 0.61 in RUL ($P <= 0.0001$, Fig. 8b). A correlation between D and θ was also found for the middle and upper lobes of both lungs, which can be seen in Fig. 8c.

Finally, the fact that Fig. 8c suggests a correlation between D and θ motivated an investigation of some theoretical relationships between these morphometric parameters. Two equations reported in the literature were examined. The first one, derived by Kamiya et al., 1974 for the minimization of volume at a bifurcation, is given by

$$\frac{D_p^2}{\sin\left(\theta_{MAJOR}+\theta_{Minor}\right)} = \frac{D_{MAJOR}^2}{\sin\theta_{MAJOR}} = \frac{D_{Minor}^2}{\sin\theta_{Minor}} \quad (4)$$

while the second, derived by Horsfield and Cumming, 1967, states that

$$\begin{cases} \cos\theta_{MAJOR} = \dfrac{D_p^4 + D_{MAJOR}^4 - D_{Minor}^4}{2 * D_p^2 * D_{Major}^2} \\ \cos\theta_{Minor} = \dfrac{D_p^4 + D_{Minor}^4 - D_{MAJOR}^4}{2 * D_p^2 * D_{Minor}^2} \end{cases} \quad (5)$$

where D_P is parent airway diameter and θ is branching angle. The validity of these relationships was examined for the two clinical groups separately for each lobe using a paired *t*-test between all parts of eq. (4) and between the experimental and theoretical results of eq. (5). However, the analysis was inconclusive, neither confirming nor rejecting the above formulas, though eq. (5) was confirmed to be valid for the branches of the airway trees that displayed higher symmetry.

DISCUSSION

Airway Tree Structure

The first part of this study deals with the methodology to extract morphometric information from HRCT images of the human lung using the commercial software PW2. The software uses validated algorithms to generate data through streamlined, automated procedures. However, there are several limitations to the quantity of the information provided without any user intervention; that is, how many airways are segmented and identified. The results of the segmentation, skeletonization, and identification of individual airways are prone to a number of artifacts due to either decreased image quality (low signal-to-noise ratio, motion) or algorithmic restrictions (multiple segmentations, leakages, and skeletonization issues), defects which are usually intensified in pathological lungs. Effects such as these can be observed in Figs. 2b–d. It has to be mentioned that a newer version of the software, which is already commercially available, is reported to obtain results deeper in the tree with much less user intervention (http://www.vidadiagnostics.com/).

The delineation of the airway tree seems to be robust down to Generation 5, especially in the lower lobes. This is shallower than the theoretically optimal resolution expected by modern HRCTs. A possible reason for this is the relatively high asymmetry at certain parts of the tree, where the minor daughter size is so much smaller than the major one that no unique segmentation is achievable. The result is often a discontinuation of airway tree segmentation, even though the distal subtree might contain several high-quality airway samples. Similarly, in regions with complicated bronchial connectivity, such as the RUL of Fig. 6a or the right subsuperior segment (RB*, Fig. 6b), the skeleton resulting from the algorithmic routine may be unrealistic. This effect can be seen in Table 2, where the trifurcations and small

TABLE 3. The main morphometric characteristics of the seven Healthy and the six asthmatic subjects per generation per lobe

		Lobar morphometric data					
		Gen	Length (mm)	Diameter (mm)	Branching angle (°)	Rotation angle (°)	Avg wall thickness (mm)
Healthy	Trachea	0	137.1 ± 21.1	18.1 ± 1			2.51 ± 0.09
	LMB	1	60.5 ± 4.3	12.61 ± 0.91	51 ± 4		2.03 ± 0.25
	RMB	1	29.0 ± 3.4	15.82 ± 1.55	44 ± 5		2.27 ± 0.33
	RMI	2	30.1 ± 2.9	12.65 ± 1.3	22 ± 2	7 ± 3	1.84 ± 0.24
	RUL	2	14.1 ± 3.6	12.68 ± 4.52	64 ± 6	7 ± 3	2.74 ± 1.75
		3	10.2 ± 3.3	6.37 ± 1.06	43 ± 15	89 ± 46	1.72 ± 0.29
		4	9.5 ± 3.3	4.5 ± 0.79	37 ± 10	93 ± 45	1.51 ± 0.41
		5	10 ± 4.1	3.35 ± 0.57	33 ±12	83 ± 37	1.39 ± 0.35
		6	9.0 ± 4	2.98 ± 0.52	34 ± 11	96 ± 45	1.49 ± 0.48
	RML	3	19.2 ± 2.7	6.49 ± 0.58	51 ± 3	92 ± 14	1.7 ± 0.23
		4	16.2 ± 8.4	4.4 ± 0.66	25 ± 6	90 ± 37	1.5 ± 0.37
		5	11.3 ± 3.6	3.44 ± 0.56	19 ± 12	87 ± 35	1.42 ± 0.29
		6	9.2 ± 4.3	2.98 ± 0.4	21 ± 14	98 ± 26	1.4 ± 0.24
	RLL	3	4.4 ± 2.4	13.01 ± 1.14	34 ± 9	92 ± 14	1.81 ± 0.25
		4	9.7 ± 2.5	7.89 ± 1.81	38 ± 12	66 ± 47	1.86 ± 0.41
		5	11.7 ± 4.9	4.68 ± 1.55	36 ± 14	78 ± 44	1.51 ± 0.33
		6	11.2 ± 4.57	4.01 ± 1.44	33 ± 12	97 ± 31	1.48 ± 0.47
		7	12.5 ± 5.9	4.19 ± 1.14	29 ± 13	107 ± 36	1.5 ± 0.33
		8	13.3 ± 4.7	3.33 ± 0.69	28 ± 10	84 ± 30	1.46 ± 0.49
		9	13.5 ± 3.5	3.04 ± 0.5	25 ± 9	75 ± 51	1.53 ± 0.21
	LUL	2	12.2 ± 3.3	10.14 ± 0.25	55 ± 13	100 ± 62	1.85 ± 0.19
		3	12.4 ± 5.7	7.66 ± 2.2	42 ± 9	80 ± 48	2.07 ± 0.63
		4	10.3 ± 5.1	5.03 ± 1.17	34 ± 15	106 ± 63	1.7 ± 0.35
		5	10 ± 3.8	4.05 ± 0.7	32 ± 15	93 ± 18	1.56 ± 0.38
		6	9.2 ± 3.6	3.62 ± 0.69	32 ± 10	85 ± 32	1.55 ± 0.47
		7	10 ± 1.7	3.46 ± 1.07	34 ±15	112 ± 21	1.56 ± 0.6
	LLL	2	13 ± 3.3	9.52 ± 1.17	28 ± 12	100 ± 62	1.76 ± 0.24
		3	13.3 ± 5.7	7.12 ± 1.18	40 ± 14	95 ± 20	1.72 ± 0.18
		4	10.3 ± 3.1	5.2 ± 1.58	38 ± 9	68 ± 51	1.68 ± 0.44
		5	10.6 ± 4.4	4.17 ± 1.41	30 ± 16	87 ± 53	1.55 ± 0.48
		6	13.6 ± 7.2	4.36 ± 0.97	30 ± 13	78 ± 47	1.78 ± 0.4
		7	12.5 ± 2.7	2.98 ± 0.53	28 ± 8	100 ± 53	1.24 ± 0.32
Asthmatics	Trachea	0	136.9 ± 5.1	18.34 ± 0.67			2.69 ± 0.19
	LMB	1	59.9 ± 4.1	12.74 ± 0.99	52 ± 6		2.05 ± 0.25
	RMB	1	27 ± 2.9	15.7 ± 1.46	44 ± 4		2.24 ± 0.43
	RMI	2	30.3 ± 1.6	11.58 ± 0.7	20 ± 6	6 ± 5	2.11 ± 0.63
	RUL	2	15.5±2.9	10.14 ± 1.58	58 ± 8	6 ± 5	2.08 ± 0.23
		3	10.4 ± 4.4	5.58 ± 1.03	43 ± 10	86 ± 32	1.79 ± 0.38
		4	10.6 ± 3.9	3.68 ± 0.73	33 ± 12	70 ± 42	1.54 ± 0.3
		5	8.7 ± 2.4	3.09 ± 0.53	31 ± 11	89 ± 43	1.5 ± 0.41
		6	6.3 ± 2	3.21 ± 0.5	30 ± 17	112 ± 28	1.61 ± 0.39
	RML	3	21.7 ± 4.1	5.74 ± 1.06	51 ± 5	93 ± 13	1.7 ± 0.18
		4	13.7 ± 5.5	4.23 ± 0.55	28 ± 9	60 ± 32	1.65 ± 0.36
		5	12.3 ± 3.1	3.35 ± 0.42	21 ± 10	75 ± 23	1.56 ± 0.29
	RLL	3	3.7 ± 2.1	10.26 ± 5.04	33 ± 8	93 ± 13	1.92 ± 0.34
		4	10.6 ± 2.6	5.95 ± 1.76	39 ± 12	80 ± 48	1.73 ± 0.16
		5	9.4 ± 5.3	4.43 ± 1.62	37 ± 16	82 ± 55	1.73 ± 0.38
		6	10.4 ±3.4	4.27 ± 1.34	32 ± 18	116 ± 34	1.62 ± 0.31
		7	11.5 ± 4.2	4.11 ± 0.92	29 ± 17	110 ± 39	1.64 ± 0.29
		8	9.8 ± 3.9	3.74 ± 0.79	32 ± 12	141 ± 21	1.62 ± 0.4
	LUL	2	11.1 ± 4.3	9.96 ± 0.43	56 ± 6	100 ± 60	1.88 ± 0.19
		3	13.5 ± 3.5	7.13 ± 1.11	39 ± 10	73 ± 48	1.85 ± 0.28
		4	12.5 ± 5.3	4.48 ± 1.28	38 ± 12	100 ± 58	1.84 ± 0.47
		5	10.0 ± 4.2	3.69 ± 0.45	35 ± 12	93 ± 39	1.71 ± 0.39
		6	8.6 ± 1.6	3.45 ± 0.5	28 ± 5	88 ± 34	1.5 ± 0.08
	LLL	2	11.6 ± 2.9	9.85 ± 2.91	26 ± 5	100 ± 60	2.3 ± 0.57
		3	14.4 ± 5.1	6.21 ± 1.54	35 ± 10	95 ± 9	1.93 ± 0.76
		4	7.2 ± 3.8	5.7 ±1.75	37 ± 13	80 ± 41	1.99 ± 0.49
		5	12.5 ± 4.4	4.5 ± 0.9	28 ± 10	81 ± 42	1.82 ± 0.44
		6	10.3 ± 5.3	3.9 ±1.1	30 ± 18	74 ± 19	1.75 ± 0.32

The lengths, diameters and avg. wall thickness are in mm, while the angles are in degrees. The morphology of the trachea, the two main bronchi and the right intermediate are provided separately. All values are mean ± STD.

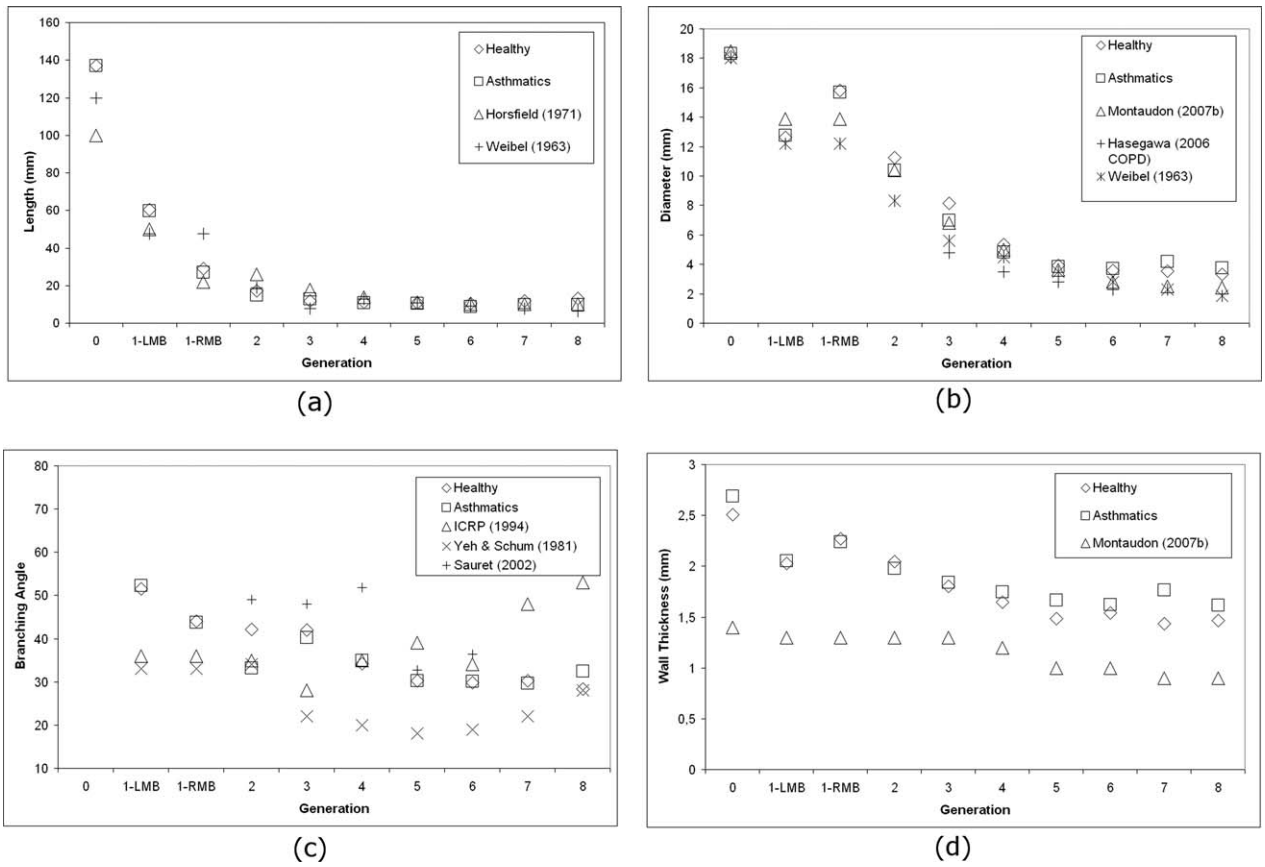

Fig. 7. Comparison of average morphometric values per generation of the Healthy and the Asthmatic group with results from the literature. **a**) Length, **b**) diameter, **c**) branching angle, and **d**) WT are the elements compared. The left and right main bronchi are provided separately and compared to Generation 1 results.

TABLE 4. The homothety ratio, least squares linear regression for the average, major and minor daughters and the L/D ratio

Homothety ratios													
Healthy													
	Average				Major daughter				Minor daughter				
	HR	Least squares			HR	Least squares			HR	Least squares			
		a	b	R^2		a	b	R^2		a	b	R^2	L/D
RUL	0.71±0.13	0.35	1.87	0.73	0.76±0.12	0.39	1.88	0.82	0.67±0.11	0.31	1.87	0.71	2.58±1.37
RML	0.72±0.09	0.56	0.82	0.64	0.78±0.08	0.6	0.81	0.71	0.67±0.07	0.51	0.78	0.79	3.39±1.48
RLL	0.71±0.14	0.5	1.11	0.64	0.78±0.13	0.63	0.83	0.75	0.64±0.12	0.38	1.39	0.74	3.11±1.7
LUL	0.73±0.13	0.58	0.92	0.61	0.8±0.12	0.72	0.5	0.68	0.67±0.1	0.44	1.35	0.76	2.36±1.22
LLL	0.73±0.14	0.72	0.07	0.66	0.8±0.14	0.84	−0.21	0.75	0.65±0.1	0.6	0.35	0.75	2.56±1.37
Asthmatics													
RUL	0.69±0.14	0.36	1.67	0.64	0.74±0.13	0.45	1.49	0.76	0.64±0.14	0.28	1.85	0.69	2.6±1.03
RML	0.72±0.08	0.58	0.76	0.64	0.75±0.07	0.58	0.87	0.68	0.69±0.08	0.57	0.65	0.66	3.53±1.25
RLL	0.73±0.17	0.34	2.22	0.37	0.84±0.13	0.48	2.08	0.61	0.62±0.13	0.2	2.36	0.43	2.59±1.58
LUL	0.69±0.13	0.62	0.43	0.65	0.74±0.13	0.69	0.25	0.7	0.64±0.12	0.54	0.61	0.67	2.54±1.23
LLL	0.77±0.18	0.39	2.52	0.27	0.86±0.16	0.48	2.51	0.38	0.69±0.15	0.3	2.53	0.25	2.17±1.16

Parameters a and b conform to the equation $y = ax + b$ representing the straight line fitted to the data while R^2 is the determination coefficient of the regression. Data are presented for generations 1–6.

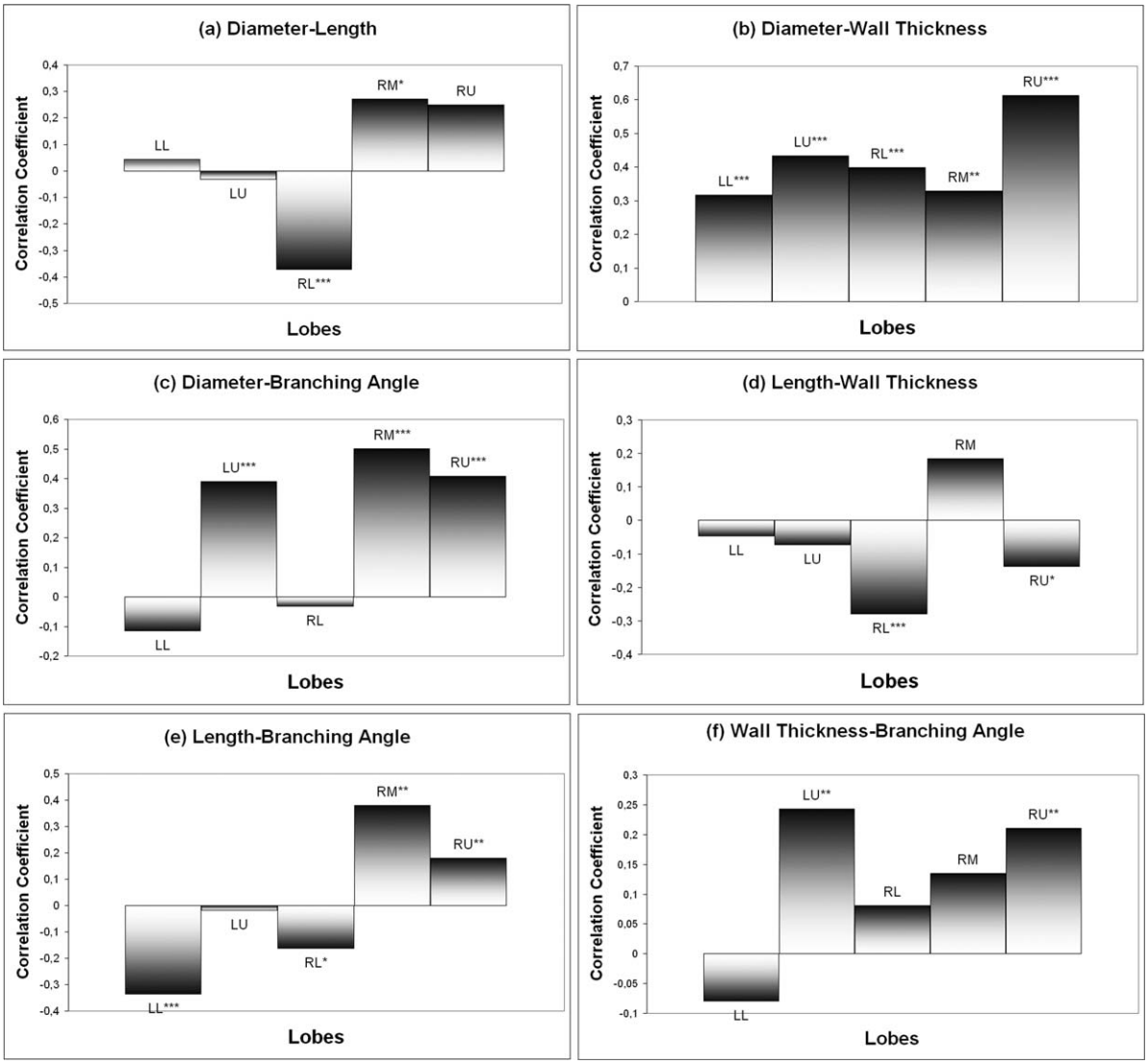

Fig. 8. Pearson correlation analysis between the morphometric parameters diameter, length, branching angle and WT. The results are presented per lobe, with $^{*}P < 0.05$, $^{**}P < 0.005$, and $^{***}P < 0.0001$.

"intermediate" airways are given per generation and per lobe. Under these conditions, the skeletonization algorithm regularly fails to delineate the airways correctly. Finally, the left lung is especially prone to motion artifacts due to proximity of the heart; these artifacts often look like low attenuation regions or "shadows" in the parenchyma. However, the expansion of the airway tree beyond this generation is possible and, indeed, required for the acquisition of additional information on airway-tree morphology. Therefore, manual intervention by the user for the optimization of the 3D reconstruction is a significant part of the process.

As mentioned earlier, since the process is semiautomatic the manual segmentation of airways might not be accurate enough. This is especially true for the asthmatic lung, where airway segmentation is less successful due to some bronchial disease characteristics. One example is the bronchial stenosis shown in Fig. 3. In some cases the lumen might not be visible at all for entire tree sections. These "invisible" subtrees are detectable intuitively, by locating subtrees that are not connected to any central airways. It is a subject for investigation whether these images represent permanent (or semipermanent) airway closures due to remodeling and inflammation of the bronchial wall (Wiggs et al., 1992; Pepe et al., 2005; Aysola et al., 2008; Zanini et al., 2010; Al-Muhsen et al., 2011), mucous plugging, or smooth muscle contraction.

Other characteristics of asthma that can affect airway segmentation include "spurs" at bifurcation points, where the lumen is compressed by increased WT, increased radius of curvature of the airways (probably due to the extra elasticity of the smooth muscle), and higher signal-to-noise ratios in the images, possibly due to extra attenuation from mucous secretions. Because of all these effects, the extraction of information from the

asthmatic images requires intuition, attention, and training on the part of the user. For that reason, a necessity exists for better algorithmic processes that eliminate user intervention to penetrate deep into the tree and quantify features such as the spurs or the levels of lumen caliber reduction. It is important to note that the 3D representation adds an important aspect to the investigation of clinically important defects, as many of the stenoses observed in our study were difficult to observe in the 2D HRCT slices.

A measure of the successful segmentation of the bronchi can be given by measuring the actual versus predicted number of airways (Table 2). These results are within the expected range of the results published by Salito et al., 2011 for images captured at residual volume (Generation 5: healthy 33% and emphysema 11%) and images acquired at total lung capacity (TLC) (Generation 6: healthy 67% and emphysema 22%). However, Montaudon et al., 2007b managed to segment more than 100% of Generation 5 airways (healthy lungs), with this percentage dropping to 84% at Generation 6 and 14% at Generation 8.

It is unclear why this discrepancy in airway detection might exist between the different techniques for similar healthy groups. The most likely reason is that the difference in breathing regimes affected the size of the bronchi, making it easier to segment out individual airways in healthy lungs at TLC. Other possible factors are algorithmic or scanning device differences. It is worth mentioning the fact that segmentation penetrates deeper in the lower lobes suggesting the possibility of positive correlation between the gravity angle (Sauret et al., 2002) and airway size.

An important finding of this work is that significant differences in airway tree structure from the theoretical bifurcating tree structure were identified (Table 2). In many cases, successive bifurcations are connected by small "intermediate" airways that may or may not be visible in the 3D object. The "intermediates" are important to the tree structure for several reasons, the most important of which is the effect they have on air flow and particle deposition, since bifurcations and trifurcations have different flow profiles (Choi et al., 2010; Gemci et al., 2008; van Ertbruggen et al., 2005). It is important to note that there is no clear delineating distinction between a trifurcation and a short child airway. An implication to tree modeling is the imbalance they cause to the number of generations in a particular subtree, causing errors of a statistical nature. Therefore, some postprocessing of the data is always necessary in order to determine the "real" connectivity and, thus, the generation of all bronchi.

A broad range of studies exists investigating the airway remodeling in different diseases (Niimi et al., 2000; Gono et al., 2003; de Jong et al., 2005; Kotaru et al., 2005; Pepe et al., 2005; Olivier et al., 2006; Aysola et al., 2008; Hoshino et al., 2010; Al-Muhsen et al., 2011). However, it is unclear if there is a higher probability for polyfurcations in different diseases. Generally speaking, there is a lack of studies in the literature correlating how diseases with genetic backgrounds affect the structure and connectivity in the airway tree or if there is a causality effect between a disease and particular types of connectivity structures. Some recent reports suggest that there is a connection between cellular dysfunction in prenatal stages of lung development and lung structure in the diseased lung postnatally, a fact that remains to be further investigated and quantified (Morrisey and Hogan, 2010). The data presented in this study fall inside the categories described by Ghaye et al., 2001, with the exception of the RM Lobe trifurcations, which has not been previously reported. However, not enough samples were available to enable any definitive conclusions.

Bronchial Morphometry

Homothety ratios. The calculated HRs, (eqs. (1)–(3)) were smaller than their theoretical optimal values (HR = 0.79 [Weibel, 1963; Horsfield and Cumming, 1967]). However, they compare very well to the values presented by Tawhai et al., 2004 and Montaudon et al., 2007b who found values closer to HR = 0.71, with Tawhai also calculating the $HR_{Major} = 0.79 \pm 0.12$ and $HR_{Minor} = 0.66 \pm 0.12$. The regression analysis performed to assess the quality of these results (Table 4) indicates that the relationships hold relatively well for all the lobes, with the exceptions of the lower lobes of the asthmatic group, where $R^2 < 0.5$. A possible explanation for this would be that the asthmatic defects are localized (King et al., 2004; Kotaru et al., 2005; Venegas et al., 2005; Tgavalekos et al., 2007) and, therefore, might be more frequent in these particular regions of the lung. What is more important, though, is that some effects such as airway stenosis or collapse seem to persist even during nonexacerbation. It is unclear if there is a rule concerning the localization of the disease effects or if there is any mathematical rule that can be used to predict the position of these defects in the lung.

Relationships between airway lengths and diameters. Another popular relationship investigated in the literature is the ratio between bronchial L and D (L/D, Table 4). The average values per generation were examined for the whole lung and the L and D appear to decline at exponential rates similar to the literature (Figs. 7a,b). The average lengths observed in our study were higher for the trachea and main bronchi (no difference found between clinical groups in ANOVA) and smaller between Generations 2–5, with convergence in deeper regions. Opposite to the length, the healthy group had a consistently higher diameter than the asthmatic group, although the difference is relatively small and statistical significance was not reached ($P = 0.066$, ANOVA). This confirms the results available in the literature, which state that the level of airway impairment is correlated to the severity of the disease (Niimi et al., 2000; Gono et al., 2003; Pepe et al., 2005; Aysola et al., 2008; Montaudon et al., 2009; Hoshino et al., 2010).

The decrease in diameter as a function of generation for the healthy group matches very well the previous literature, but our set is consistently higher in absolute values. This was unexpected since image acquisition was performed below TLC in our study as compared to TLC in the literature. Due to lack of more information, this type of effect cannot be assessed. Another possibility for the discrepancies between the diameter results is the different algorithms used for the calculation of the morphometric information.

The issues presented above indicate that there is a need for standard protocols for image acquisition and standardization concerning the algorithms and tools utilized for morphometric measurements. It has to be noted that the differences observed for Generation 6 and deeper can probably be attributed to the small number of samples at this lung depth. At Generation 5, where an adequate number of airways are detectable, there appears to be convergence between all datasets for both length and diameter.

The average values of L/D ratios calculated in this study, ranging between 2.4 and 3.5 with average std of ~1.3 (Table 4), correspond well with those presented by Phillips and Kaye, 1995 ($L/D_{MAJOR} = 2.71 \pm 1.13$ and $L/D_{Minor} = 2.96 \pm 0.97$) but not as well with other studies, which predict higher average L/D ratios. For example, Tawhai et al., 2004 calculated $L/D = 3.04 \pm 2.20$ (Multi Detector CT) and 2.92 ± 0.92 (Model), Sauret et al., 2002 calculated $L/D = 3.09 \pm 1$ (HRCT), Weibel, 1963 found a value ranging between 2.8–3.25 while Kitaoka's model (Kitaoka et al., 1999) predicts a ratio between 2.94 ± 0.35 and 3.17 ± 0.56.

The high L/D variability in our and the Tawhai studies can be partially explained by observing the results in different lobes (Table 3). Airway diameter decreases exponentially in all lobes where this is not true for the length, which displays higher variability. In addition, no statistical correlation was found between L and D in any lung location other than the RLL (Fig. 8a). This result suggests the importance of adhering to local rules for airway tree modeling, since the average values often used in the literature imply trends that may be misleading and could possibly not be applicable on a local basis.

Relationships between diameter and WT. Relationships between the airway lumen diameter and the WT have been well documented in the past for both healthy and diseased lungs (ICRP, 1994; Niimi et al., 2000; Gono et al., 2003; Hasegawa et al., 2006; Montaudon et al., 2007a, b; Aysola et al., 2008; Montaudon et al., 2009; Hoshino et al., 2010; Politi et al., 2010). Figure 8b, displaying the results of the ANOVA analysis per lobe, confirms that such a correlation between the two morphometric characteristics exists and is statistically significant, though it might be somewhat less strong than indicated in the literature. However, WT is relatively difficult to measure either manually or through measurements performed on CT images. For that reason, some studies concentrated on particular representative airways such as the right upper appical segment (Niimi et al., 2000; Gono et al., 2003; Robinson et al., 2009; Hoshino et al., 2010). As WT is very dependent on the algorithms used when obtained from automatic measurements (de Jong et al., 2005) not much data describing the WT throughout the bronchial tree have been published. The problem is illustrated through the graph of Fig. 7d, where our results are compared to the data given by Montaudon et al., 2007b. The relatively large difference between the two sets can only be attributed to the different methods used for the calculation of the WT, which amplifies the point made earlier concerning the use of common methodologies during data acquisition. It also has to be noted that the consistent difference between the healthy and the asthmatic groups confirms the hypothesis that predicts thicker bronchial walls for asthmatic patients (Niimi et al., 2000; Gono et al., 2003; Aysola et al., 2008; Montaudon et al., 2009; Hoshino et al., 2010).

Branching angle θ**.** The last morphometric characteristic examined in this study is the branching angle, which is plotted in Fig. 7c for a comparison between the two groups and some datasets available in the literature. The healthy and the asthmatic groups are very similar, with the only difference in Generation 2. However, the results are different to the literature data, with less variability between different generations and relatively close to the optimal value of 37° as calculated by Horsfield and Cumming, 1967 and Kamiya et al., 1974.

Several factors may be responsible for these differences, with the most likely being the different measurement methods used. For example, the data presented by Yeh and Schum, 1980, based on the Lovelace data produced by Phalen et al., 1978, are based on manual measurements made on lung casts, which are known to be prone to deformation errors (Phalen et al., 1985; Sauret et al., 2002). Furthermore, manual measurements are frequently biased and have very low repeatability due to their unsystematic nature. Another important factor is the relatively small datasets studied, a fact which tends to exaggerate the intrasubject compared to intersubject variation. This is better displayed when the lobar angles per generation (Table 3) are superimposed to the automatic measurements of Sauret et al., 2002, with our data displaying a much more "regular" behavior having values in the expected limits between 30° and 40°. The treatment of trifurcations and "intermediate" airways may play an important role in the average values recorded in each study. Finally, the degree to which the breathing patterns in health and disease affect branching angle is also something that may be worth investigating.

It has to be mentioned that substantive conclusions can be drawn for θ data only up to Generation 6, since after this generation the dataset becomes very sparse and is primarily dominated by the lower lobes. Because of the weak negative correlation between length and branching angle for the lower lobes (Fig. 8e), the slightly larger lengths observed in those regions can account for the relatively small angles after Generation 6, which are measured to be close to 30°. These are expected to rise to values closer to 50° in deeper parts of the lung where gas transport stops being the dominant bronchial tree function, probably following a curve similar to the International Commission on Radiological Protection (ICRP) data (ICRP, 1994).

The fact that the optimality relationships expressed by eqs. (4) and (5) are not found to be valid at the observable depth underlines the necessity for more datasets to become available in order to work out new rules based on a broader range of systematically obtained experimental data. Where tree-modeling is concerned, the use of eq. (4) by Kitaoka et al., 1999 was shown to generate a bronchial tree displaying a higher degree of asymmetry compared to the human lung. Furthermore, Tawhai et al., 2004 provided branching angle data for diameter ranges but no distinction was made to the

location where the data are measured and, as discussed above, variations appear to exist between different lobes. It is also worth noting that no angular data exist in the literature for diseased lungs. We feel that this is an important omission, since the remodeling occurring in the bronchial tissue (Pepe et al., 2005; Aysola et al., 2008; Politi et al., 2010; Zanini et al., 2010; Al-Muhsen et al., 2011) because of the disease affects the elasticity of the airways, thus also affecting their orientation between different body positions and during different breathing conditions.

Modeling implications. It becomes obvious from the results presented above that in patients with asthma the average values per generation are not descriptive enough to express the full measure of airway dysfunction. For example, computational fluid dynamic simulations and interpretation of particle deposition images (SPECT/PET) may vary considerably with the detection of features such as stenoses or trifurcations. What is more, better relationships and methods of detecting, predicting and expressing local features and defects are necessary for the more accurate modeling of the airway tree in both health and disease. Furthermore, since the morphometric data are dependent on the algorithmic methods used for airway segmentation and measurements, a meaningful comparison between different datasets would require either one of two conditions to be true: (1) all the studies should be performed using the same or equivalent algorithms or (2) the differences between the algorithms are clearly understood and, if possible, quantified.

In summary, our current study did not reveal many trends or big differences between the healthy and the asthmatic group with any severe modeling implications. Both groups display equivalent diameter rates of decline with airway generation, with the healthy diameter slightly higher. The WT has a significant correlation to D and is larger in the asthmatic group, as expected due to remodeling. However, the L and θ values did not seem to follow any established trend in different locations in the lung. Furthermore, the HR values might be similar between the groups, but with significant variability in the asthmatic population which is displayed by the bad quality of the linear regression performed. Finally, the number of samples was too small for any general trends to be observed concerning structural connectivity and the presence of polyfurcations.

CONCLUSIONS

This article was concerned with two themes. The first is a description of how HRCT and any automatic segmentation software, such as PW2, provide a powerful methodology for studying airway morphology. However, the methodology is shown to still be heavily dependent on user intervention, thus somewhat reducing the reproducibility and systematic character of the results. For that reason, it is important for better, more stream-lined methods to become available for use, especially since these tools can be invaluable for the study of disease and clinical applications, where disease imposes additional limitations to the current software.

The second theme of this article is the study of the airway tree as obtained through the particular methodologies and the investigation of the results in the context of mathematical modeling. The structure of the bronchial tree is highly variable; however, there is no quantification on the degree to which it is affected by disease, especially regarding the trifurcations and the "intermediate" airways. This suggests that a description of airway structure in terms of regular bifurcations needs to be updated. Furthermore, the first five generations of different parts of the lung seem to have different morphometric characteristics. These two issues are important when models of the airway tree are formulated, since a common practice in the literature is to follow rules based on a strictly bifurcating structure expanding similarly to the whole lung, which can be shown to be a misleading practice.

Finally, the study of some morphometric characteristics of moderate persistent asthma was attempted. Some trends and differences between health and disease could be established and compared with previously published data; however, more information is necessary to establish definitive rules that can be systematically reproduced when modeling the disease.

LITERATURE CITED

Al-Muhsen S, Johnson JR, Hamid Q. 2011. Remodeling in asthma. J Allergy Clin Immunol 128:451–462.

Aysola RS, Hoffman EA, Gierada D, Wenzel S, Cook-Granroth J, Tarsi J, Zheng J, Schechtman KB, Ramkumar TP, Cochran R, Xueping E, Christie C, Newell J, Fain S, Altes TA, Castro M. 2008. Airway remodeling measured by multidetector CT is increased in severe asthma and correlates with pathology. Chest 134:1183–1191.

Choi J, Xia G, Tawhai MH, Hoffman EA, Lin CL. 2010. Numerical study of high-frequency oscillatory air flow and convective mixing in a CT-based human airway model. Ann Biomed Eng 38:3550–3571.

Conway J, Fleming J, Majoral C, Katz I, Perchet D, Peebles C, Tossici-Bolt L, Collier L, Caillibotte G, Pichelin M, Sauret-Jackson V, Martonen T, piou-Sbirlea G, Muellinger B, Kroneberg P, Gleske J, Scheuch G, Texereau Jl, Martin A, Montesantos S, Bennett M. 2012. Controlled, parametric, individualized, 2-D and 3-D imaging measurements of aerosol deposition in the respiratory tract of healthy human subjects for model validation. J Aerosol Sci 52:1–17.

Coxson HO, Mayo J, Lam S, Santyr G, Parraga G, Sin DD. 2009. New and current clinical imaging techniques to study chronic obstructive pulmonary disease. Am J Respir Crit Care Med 180:588–597.

Darquenne C, van Ertbruggen C, Prisk GK. 2011. Convective flow dominates aerosol delivery to the lung segments. J Appl Physiol 111:48–54.

de Jong PA, Muller NL, Pare PD, Coxson HO. 2005. Computed tomographic imaging of the airways: relationship to structure and function. Eur Respir J 26:140–152.

Eberle B, Weiler N, Vogel N, Kauczor HU, Heinrichs W. 1999. Computed tomography-based tracheobronchial image reconstruction allows selection of the individually appropriate double-lumen tube size. J Cardiothorac Vasc Anesth 13:532–537.

Fleming J, Conway J, Majoral C, Tossici-Bolt L, Katz I, Caillibotte G, Perchet D, Pichelin M, Muellinger B, Martonen T, Kroneberg P, piou-Sbirlea G. 2011. The use of combined single photon emission computed tomography and X-ray computed tomography to assess the fate of inhaled aerosol. J Aerosol Med Pulm Drug Deliv 24:49–60.

Fleming JS, Nassim M, Hashish AH, Bailey AG, Conway H, Holgate S, Halson P, Moore E, Martonen TB. 1995. Description of pulmonary deposition of radiolabeled aerosol by airway

generation using a conceptual three dimensional model of lung morphology. J Aerosol Med 8:341–356.

Freitas RK, Schroder W. 2008. Numerical investigation of the three-dimensional flow in a human lung model. J Biomech 41:2446–2457.

Gemci T, Ponyavin V, Chen Y, Chen H, Collins R. 2008. Computational model of airflow in upper 17 generations of human respiratory tract. J Biomech 41:2047–2054.

Ghaye B, Szapiro D, Fanchamps JM, Dondelinger RF. 2001. Congenital bronchial abnormalities revisited. Radiographics 21:105–119.

Gono H, Fujimoto K, Kawakami S, Kubo K. 2003. Evaluation of airway wall thickness and air trapping by HRCT in asymptomatic asthma. Eur Respir J 22:965–971.

Hasegawa M, Nasuhara Y, Onodera Y, Makita H, Nagai K, Fuke S, Ito Y, Betsuyaku T, Nishimura M. 2006. Airflow limitation and airway dimensions in chronic obstructive pulmonary disease. Am J Respir Crit Care Med 173:1309–1315.

Horsfield K, Cumming G. 1967. Angles of branching and diameters of branches in the human bronchial tree. Bull Math Biophys 29:245–259.

Horsfield K, Dart G, Olson DE, Filley GF, Cumming G. 1971. Models of the human bronchial tree. J Appl Physiol 31:207–217.

Hoshino M, Matsuoka S, Handa H, Miyazawa T, Yagihashi K. 2010. Correlation between airflow limitation and airway dimensions assessed by multidetector CT in asthma. Respir Med 104:794–800.

ICRP. 1994. Publication 66. Human respiratory tract model for radiological protection. Pergamon: ICRP.

Kamiya A, Togawa T, Yamamoto A. 1974. Theoretical relationship between the optimal models of the vascular tree. Bull Math Biol 36:311–323.

Katz IM, Martin AR, Muller PA, Terzibachi K, Feng CH, Caillibotte G, Sandeau J, Texereau J. 2011. The ventilation distribution of helium-oxygen mixtures and the role of inertial losses in the presence of heterogeneous airway obstructions. J Biomech 44:1137–1143.

Kauczor HU. 2003. Hyperpolarized helium-3 gas magnetic resonance imaging of the lung. Top Magn Reson Imaging 14:223–230.

King GG, Carroll JD, Muller NL, Whittall KP, Gao M, Nakano Y, Pare PD. 2004. Heterogeneity of narrowing in normal and asthmatic airways measured by HRCT. Eur Respir J 24:211–218.

Kitaoka H, Takaki R, Suki B. 1999. A three-dimensional model of the human airway tree. J Appl Physiol 87:2207–2217.

Kotaru C, Coreno A, Skowronski M, Muswick G, Gilkeson RC, McFadden ER, Jr. 2005. Morphometric changes after thermal and methacholine bronchoprovocations. J Appl Physiol 98:1028–1036.

Lewis TA, Tzeng YS, McKinstry EL, Tooker AC, Hong K, Sun Y, Mansour J, Handler Z, Albert MS. 2005. Quantification of airway diameters and 3D airway tree rendering from dynamic hyperpolarized 3He magnetic resonance imaging. Magn Reson Med 53:474–478.

Lin CL, Tawhai MH, McLennan G, Hoffman EA. 2009. Computational fluid dynamics. IEEE Eng Med Biol Mag 28:25–33.

Martonen TB, Yang Y, Hwang D, Fleming JS. 1995. Computer model of human lung morphology to complement SPECT analyses. Int J Biomed Comput 40:5–16.

Montaudon M, Berger P, Cangini-Sacher A, de Dietrich G, Tunon-de-Lara JM, Marthan R, Laurent F. 2007a. Bronchial measurement with three-dimensional quantitative thin-section CT in patients with cystic fibrosis. Radiology 242:573–581.

Montaudon M, Desbarats P, Berger P, de Dietrich G, Marthan R, Laurent F. 2007b. Assessment of bronchial wall thickness and lumen diameter in human adults using multi-detector computed tomography: comparison with theoretical models. J Anat 211:579–588.

Montaudon M, Lederlin M, Reich S, Begueret H, Tunon-de-Lara JM, Marthan R, Berger P, Laurent F. 2009. Bronchial measurements in patients with asthma: comparison of quantitative thin-section CT findings with those in healthy subjects and correlation with pathologic findings. Radiology 253:844–853.

Montesantos S, Fleming JS, Tossici-Bolt L. 2010. A spatial model of the human airway tree: the hybrid conceptual model. J Aerosol Med Pulm Drug Deliv 23:59–68.

Morrisey EE, Hogan BL. 2010. Preparing for the first breath: genetic and cellular mechanisms in lung development. Dev Cell 18:8–23.

Niimi A, Matsumoto H, Amitani R, Nakano Y, Mishima M, Minakuchi M, Nishimura K, Itoh H, Izumi T. 2000. Airway wall thickness in asthma assessed by computed tomography. Relation to clinical indices. Am J Respir Crit Care Med 162:1518–1523.

Olivier P, Hayon-Sonsino D, Convard JP, Laloe PA, Fischler M. 2006. Measurement of left mainstem bronchus using multiplane CT reconstructions and relationship between patient characteristics or tracheal diameters and left bronchial diameters. Chest 130:101–107.

Pepe C, Foley S, Shannon J, Lemiere C, Olivenstein R, Ernst P, Ludwig MS, Martin JG, Hamid Q. 2005. Differences in airway remodeling between subjects with severe and moderate asthma. J Allergy Clin Immunol 116:544–549.

Peterson ET, Dai J, Holmes JH, Fain SB. 2011. Measurement of lung airways in three dimensions using hyperpolarized helium-3 MRI. Phys Med Biol 56:3107–3122.

Phalen RF, Oldham MJ, Beaucage CB, Crocker TT, Mortensen JD. 1985. Postnatal enlargement of human tracheobronchial airways and implications for particle deposition. Anat Rec 212:368–380.

Phalen RF, Yeh HC, Schum GM, Raabe OG. 1978. Application of an idealized model to morphometry of the mammalian tracheobronchial tree. Anat Rec 190:167–176.

Phillips CG, Kaye SR. 1995. Diameter-based analysis of the branching geometry of four mammalian bronchial trees. Respir Physiol 102:303–316.

Phillips CG, Kaye SR, Schroter RC. 1994. A diameter-based reconstruction of the branching pattern of the human bronchial tree. Part I. Description and application. Respir Physiol 98:193–217.

Politi AZ, Donovan GM, Tawhai MH, Sanderson MJ, Lauzon AM, Bates JH, Sneyd J. 2010. A multiscale, spatially distributed model of asthmatic airway hyper-responsiveness. J Theor Biol 266:614–624.

Robinson RJ, Russo J, Doolittle RL. 2009. 3D airway reconstruction using visible human data set and human casts with comparison to morphometric data. Anat Rec 292:1028–1044.

Salito C, Barazzetti L, Woods JC, Aliverti A. 2011. 3D airway tree reconstruction in healthy subjects and emphysema. Lung 189:287–293.

Sauret V, Halson PM, Brown IW, Fleming JS, Bailey AG. 2002. Study of the three-dimensional geometry of the central conducting airways in man using computed tomographic (CT) images. J Anat 200:123–134.

Schmidt A, Zidowitz S, Kriete A, Denhard T, Krass S, Peitgen HO. 2004. A digital reference model of the human bronchial tree. Comput.Med.Imaging Graph 28:203–211.

Seneterre E, Paganin F, Bruel JM, Michel FB, Bousquet J. 1994. Measurement of the internal size of bronchi using high resolution computed tomography (HRCT). Eur Respir J 7:596–600.

Soong TT, Nicolaides P, Yu CP, Soong SC. 1979. A statistical description of the human tracheobronchial tree geometry. Respir Physiol 37:161–172.

Tawhai MH, Hunter P, Tschirren J, Reinhardt J, McLennan G, Hoffman EA. 2004. CT-based geometry analysis and finite element models of the human and ovine bronchial tree. J Appl Physiol 97:2310–2321.

Tgavalekos NT, Musch G, Harris RS, Vidal Melo MF, Winkler T, Schroeder T, Callahan R, Lutchen KR, Venegas JG. 2007. Relationship between airway narrowing, patchy ventilation and lung mechanics in asthmatics. Eur Respir J 29:1174–1181.

Tzeng YS, Hoffman E, Cook-Granroth J, Gereige J, Mansour J, Washko G, Cho M, Stepp E, Lutchen K, Albert M. 2008. Investigation of hyperpolarized 3He magnetic resonance imaging utility in examining human airway diameter behavior in asthma through comparison with high-resolution computed tomography. Acad Radiol 15:799–808.

van Ertbruggen C, Hirsch C, Paiva M. 2005. Anatomically based three-dimensional model of airways to simulate flow and particle transport using computational fluid dynamics. J Appl Physiol 98:970–980.

Venegas JG, Winkler T, Musch G, Vidal Melo MF, Layfield D, Tgavalekos N, Fischman AJ, Callahan RJ, Bellani G, Harris RS. 2005. Self-organized patchiness in asthma as a prelude to catastrophic shifts. Nature 434:777–782.

Weibel ER. 1963. Morphometry of the human lung. Heidelberg: Springer-Verlag.

Wiggs BR, Bosken C, Pare PD, James A, Hogg JC. 1992. A model of airway narrowing in asthma and in chronic obstructive pulmonary disease. Am Rev Respir Dis 145:1251–1258.

Yeh HC, Schum GM. 1980. Models of human lung airways and their application to inhaled particle deposition. Bull Math Biol 42:461–480.

Zanini A, Chetta A, Imperatori AS, Spanevello A, Olivieri D. 2010. The role of the bronchial microvasculature in the airway remodelling in asthma and COPD. Respir Res 11:132.